Boosting the K^+-adsorption capacity in edge-nitorgen doped hierarchically porous carbon spheres for ultrastable potassium ion battery anodes

Yang Xu,[a,b,cΔ] Xinpeng Sun,[a,b,cΔ] Zhiqiang Li,[a,b,c] Lingzhi Wei,[a,b,c] Ge Yao,[a,b,c] Heling Niu,[c] Yang Yang,[d*] Fangcai Zheng [a,b,c*] and Qianwang Chen[d]

[a]Institutes of Physical Science and Information Technology, Key Laboratory of Structure and Functional Regulation of Hybrid Materials of Ministry of Education, Anhui University, Hefei, 230601, China

[b]Anhui Graphene Engineering Laboratory, Anhui University, Hefei, 230601, China

[c] Anhui Province Key Laboratory of Chemistry for Inorganic/Organic Hybrid Functionalized Materials, Energy Materials and Devices Key Laboratory of Anhui Province for Photoelectric Conversion, Anhui University, Hefei, 230601, China

[d]Hefei National Laboratory for Physical Science at Microscale and Department of Materials Science & Engineering, University of Science and Technology of China, Hefei, 230026, China

Corresponding authors:yangyang@1991.ustc.edu.cn (Y. Yang)

zfcai@mail.ustc.edu.cn (F.C. Zheng)

[Δ] These authors contribute equally to this work.

Experiment

Material Synthesis

Ferrocene ($Fe(C_5H_5)_2$, ≥98%), acetone (C_3H_6O, ≥98.5%), 30% hydrogen peroxide (H_2O_2), commerically active carbon (AC) and ultrawater were used. All reagents are analytically pure without any further purification.

The Fe_3O_4@C was synthesized by a simple solvothermal method. Firstly, 0.3 g of ferrocene was ultrasonically dissolved in 30 mL of acetone in 50 mL Teflon-lined stainless steel autoclave, and then 2 mL of H_2O_2 was added the above solution after stirred 30 min. The stainless steel autoclave was heated at 200 °C for 48 h. The product was collected by centrifugation, washed with acetone for three times, and dried at 60 ℃ overnight.[1] The as-prepared precursor was placed in ceramic boat and annealed at 600 ℃ in N_2 with a heating rate of 5 ℃ min^{-1}, which was kept for 2 h. Subsequently, the as-prepared Fe_3O_4@C was stirred for 6 h in acid (3 mol/L HCl solution) at room temperature to remove Fe_3O_4. The corresponding samples were denoted as PCs. And, PCs was further placed in ceramic boat, which was annealed at 500 ℃, 600 ℃, 700 ℃ for 4 hours in NH_3 with a heating rate of 5 ℃ min^{-1}, respectively. The resulting samples were correspondingly denoted as ENPCs-500, ENPCs-600 and ENPCs-700.

For the synthesis of NSCs, 40 mL of 1.0 mol/L glucose aqueous solution was added into a 50 mL Teflon-lined stainless steel autoclave. The furnace was maintained at 180 °C for 24 h, and then cooled to room temperature naturally. The obtained product was washed by ethanol for three times and dried at 60 °C. Then, the product was carbonized in N_2 600 °C for 2h, and the carbonized sample was further calcinated in NH_3 at 600 °C for 4 h to obtain nitrogen-doped solid carbon spheres (NSCs).

Material Characterization

All the samples (PCs, NSCs-600, ENPCs-500, ENPCs-600 and ENPCs-700) were tested with a X-ray power diffraction (XRD) (Rigaku Co, Japan, D/MAX-γA). The morphology of samples was observed by scanning electron microscopy (SEM, JEOL JSM-6700 M). Transmission electron microscopy (TEM, Hitachi H-800) and high resolution transmission electron microscopy (HRTEM, JEOL-2011) was employed to observe the internal structure of material and the element distribution. The electronic states and element valence of related elements were characterized by X-ray photoelectron spectroscopy (XPS). The degree of defect and graphetic of porous carbon was characterized by Raman spectra (Via-Reflex/inVia-Reflex). A Shimadzu-50 thermoanalyser (TGA) was used to study the thermal process of the Fe_3O_4@C under flowing N_2 with a heating rate of 20 ℃ min^{-1} from the room temperature to 900 ℃.

Electrochemical Measurements

The cell was assembled with CR2032 coin cells in a glovebox filled with Argon atmosphere (O_2≤0.01 ppm, H_2O≤0.01 ppm). To prepare the electrode, acetylene black and Polyvinylidene Fluoride (PVDF) were mixed at ratio of 8:1:1 in N-methyl pyrrolidone (NMP) to form uniform slurry. The slurry was loaded on the Cu foil and then dried at 80 °C for 24 h in a vacuum drying oven. The pure metal potassium is employed as the cathode electrode, and the electrolyte was a solution of 3 mol L^{-1} KFSI in EC:DC = 1:1. The loading mass of electrode materials is about 0.5 mg cm^{-2}. For potassium ion capacitors, ENPCs-600 coated on Al foil was served as the anode and commercial activated carbon (Alladdin) was served as the cathode. The mass ratio for anode and cathode is 1:1.5. Cyclic voltammetry (CV) and electrochemical impedance spectroscopy (EIS) were performed on CHI760E electrochemical

workstation. The galvanostatic charge/discharge measurements and Galvanostatic Intermittent Titration Technique were conducted on Neware CT3008W.

Theoretical calculations

The generalized gradient approximation (GGA) of Perdew-Becke-Ernzerh of (PBE) is used for the exchange-correlation functional.[2] The conjugate gradient algorithm was used in the structural optimization, providing a convergence of 10^{-5} eV in total energy and 0.02 eV $Å^{-1}$ in Hellmann Feynman force on each atom. The atomic structures are fully relaxed in all calculations. To ensure the accuracy of the calculated results, the cutoff energy was set to high enough, 450 eV. The Monkhorst-Pack Scheme with $5 \times 5 \times 1$ K-point mesh is used to represent the Brillouin zone for structure optimization. To understand the interaction mechanism of K^+ and doped grapehene, we also calculate the K^+ adsorption energy (ΔE_a).[3] The adsorption (binding) energy of the K atoms was evaluated from $\Delta E_a = E_{GK} - (E_G + E_K)$ where E_{GK} and E_G are the energies of doped graphene models after K adsorption and without adsorption, respectively. Van der Waals corrections were considered in the calculations.

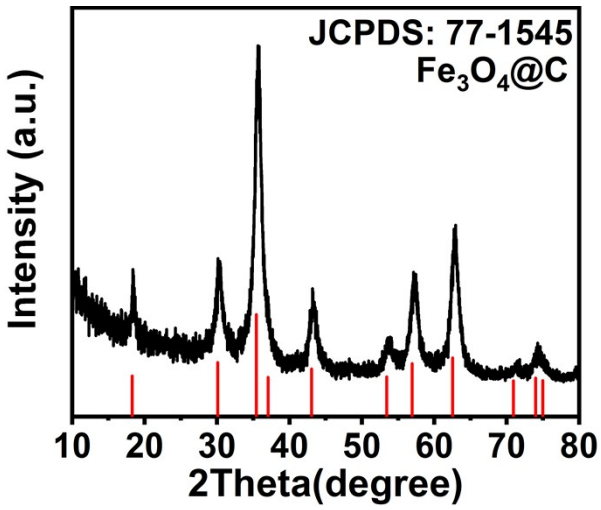

Figure S1. The XRD pattern of Fe_3O_4@C.

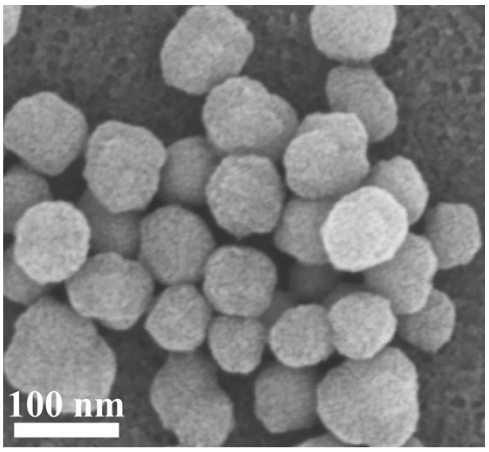

Figure S2. The SEM image of Fe_3O_4 @C.

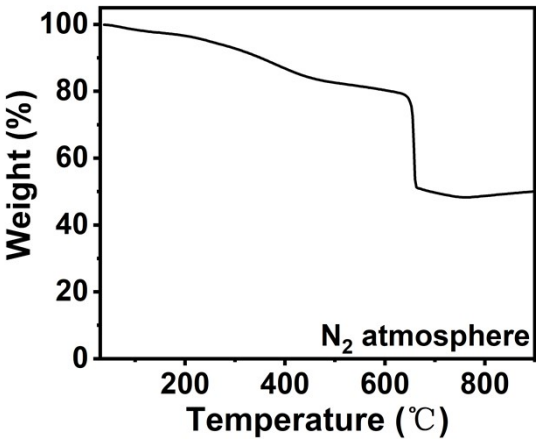

Figure S3. The TG curve of Fe_3O_4 @C.

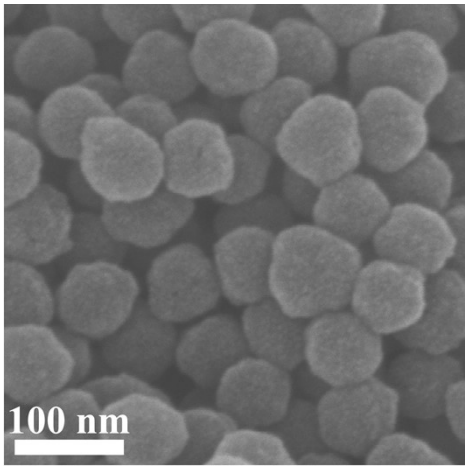

Figure S4. The SEM image of ENPCs-600.

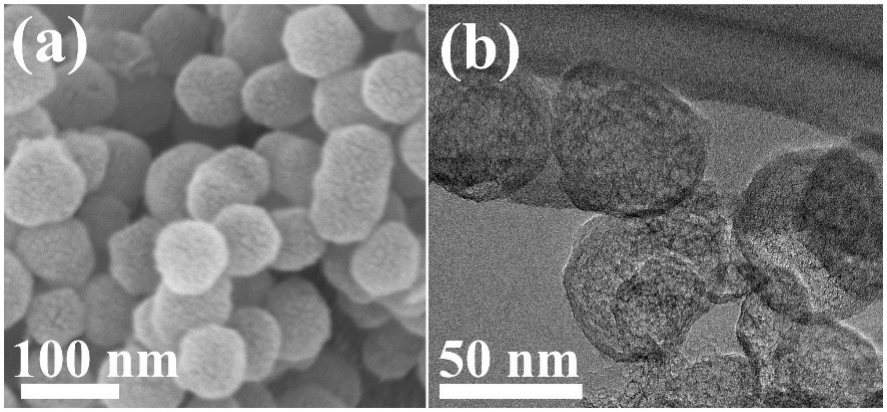

Figure S5. SEM and TEM images of ENPCs-500.

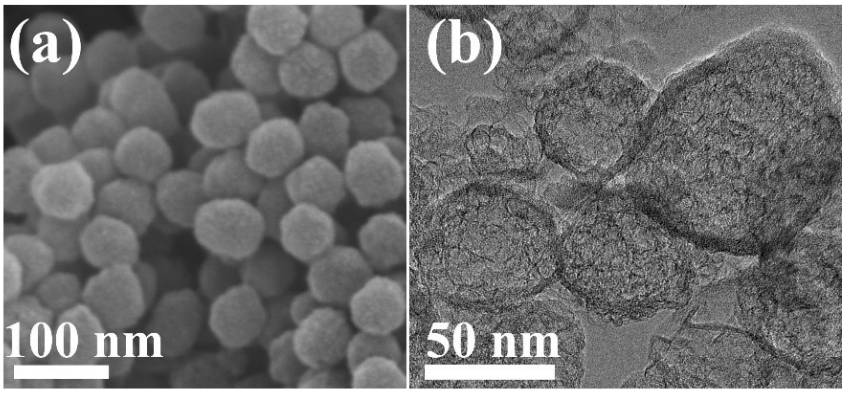

Figure S6. SEM and TEM images of ENPCs-700.

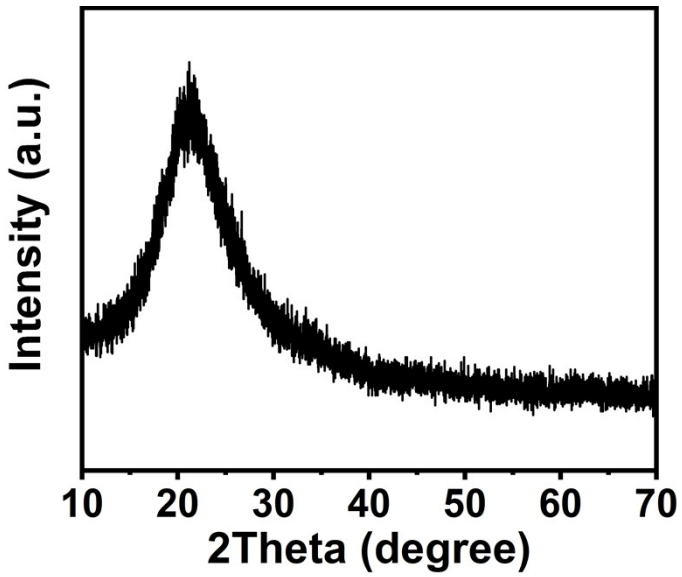

Figure S7. The XRD pattern of the glucose-derived carbon materials.

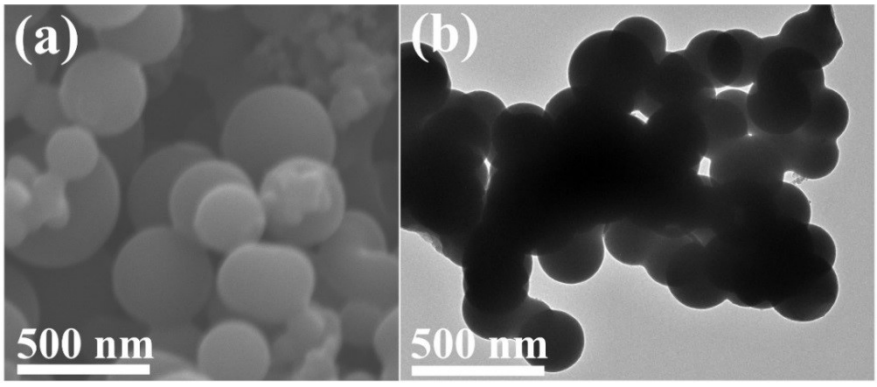

Figure S8. SEM and TEM images of glucose-derived carbon materials.

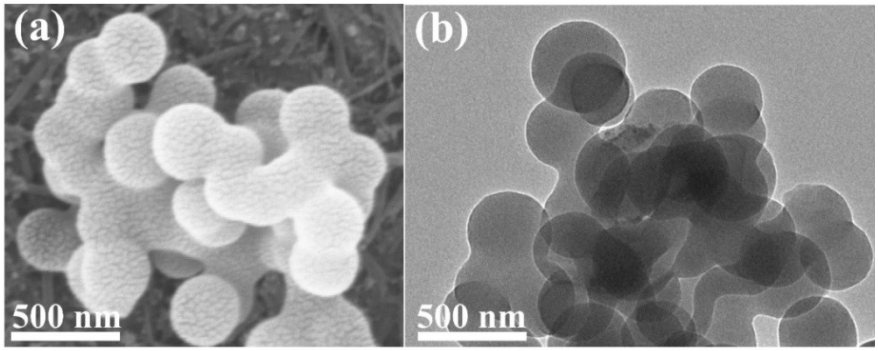

Figure S9. SEM and TEM images of NSCs.

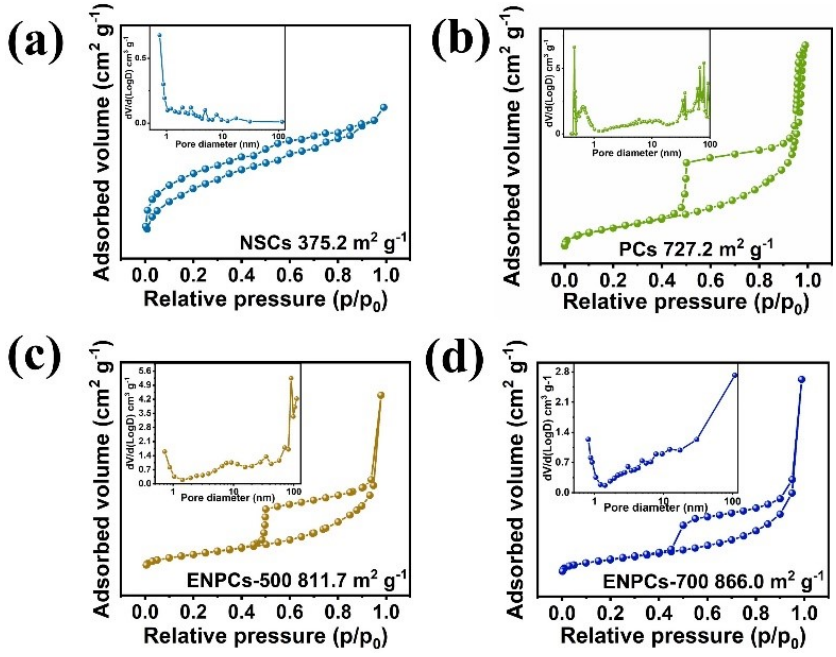

Figure S10. The N_2 adsorption/desorption isotherm curves of (a) NSCs, (b) PCs, (c) ENPCs-500, and (d) ENPCs-700.

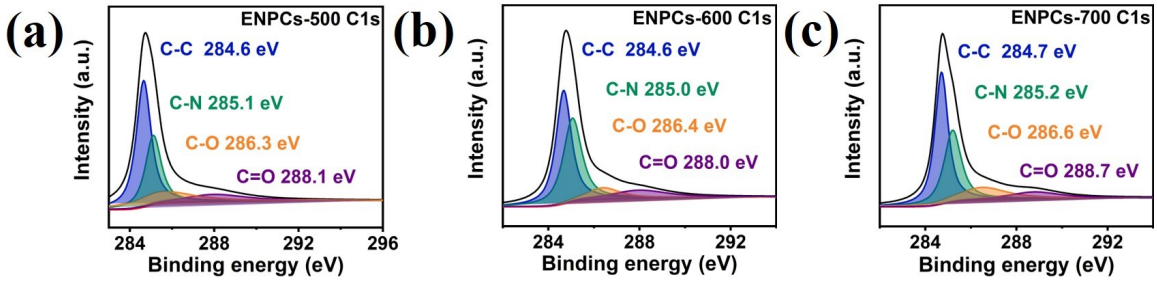

Figure S11. C1s spectra of (a) EPNCs-500, (b) EPNCs-600 and (c) EPNCs-700.

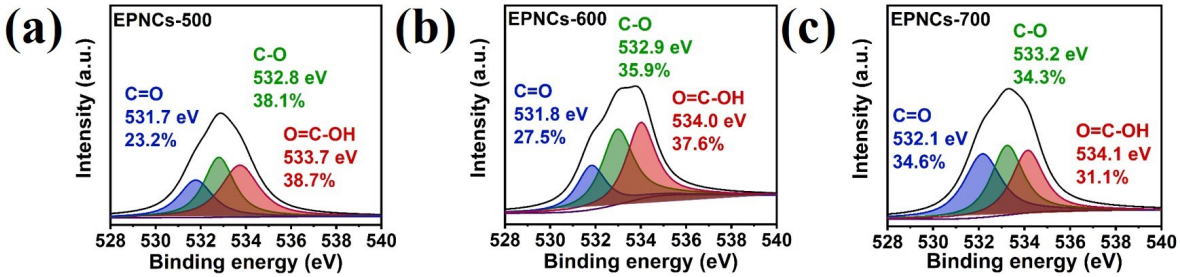

Figure S12. O1s spectra of (a) EPNCs-500, (b) EPNCs-600 and (c) EPNCs-700.

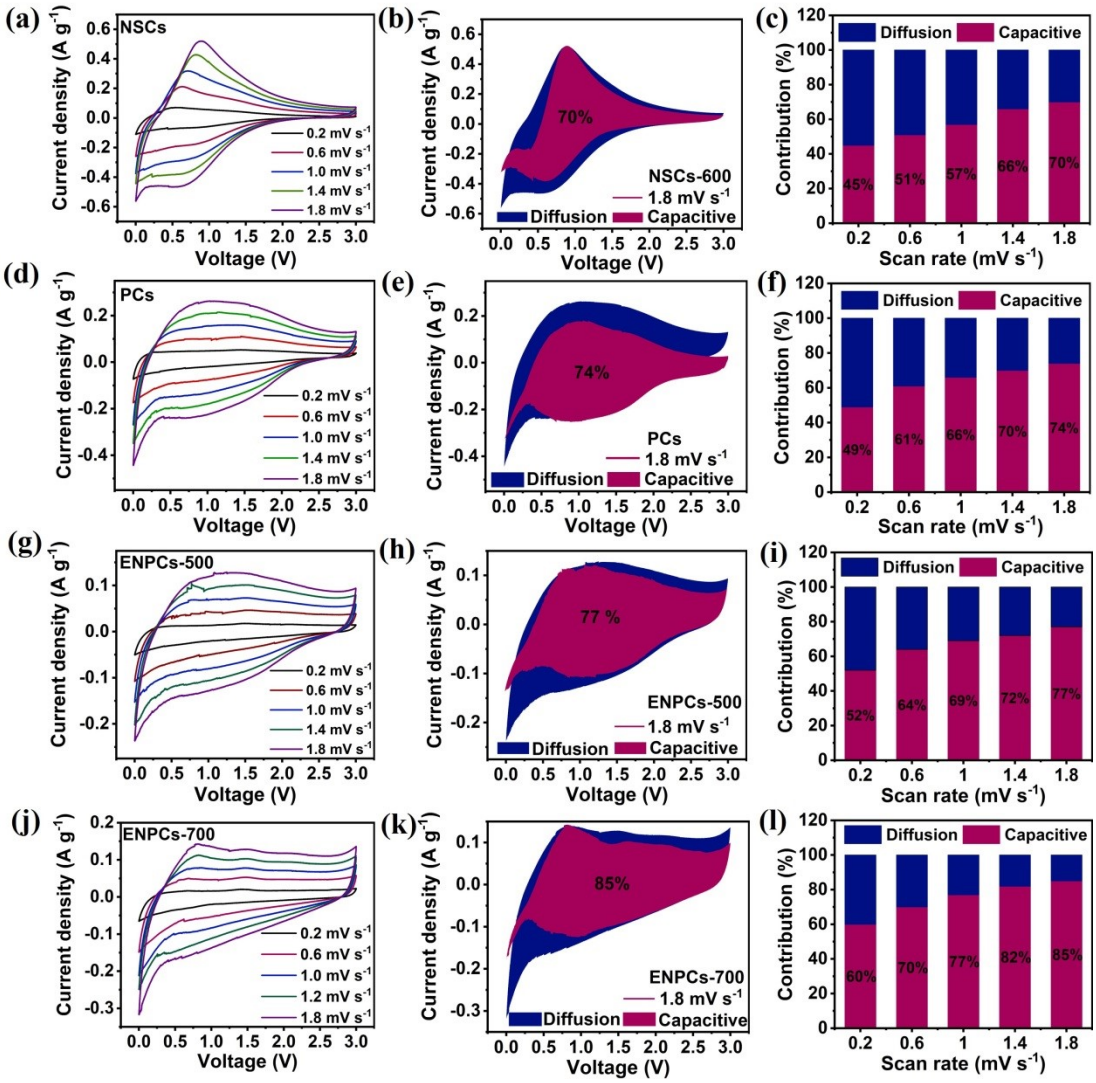

Figure S13. Quantitative analysis of surface-dominated potassium storage. CV curves of (a) NSCs, (d) PCs, (g) ENPCs-500, and (j) ENPCs-700 at different scan rates of 0.2-1.8 mV s^{-1}. Capacitive charge-storage contribution in the (b) NSCs, (e) PCs, (h) ENPCs-500, and (k) ENPCs-700 at a scan rate of 1.8 mV s^{-1}. Contribution ratios of the capacitive process in the (c) NSCs, (f) PCs, (i) ENPCs-500, and (l) ENPCs-700 at different scan rates.

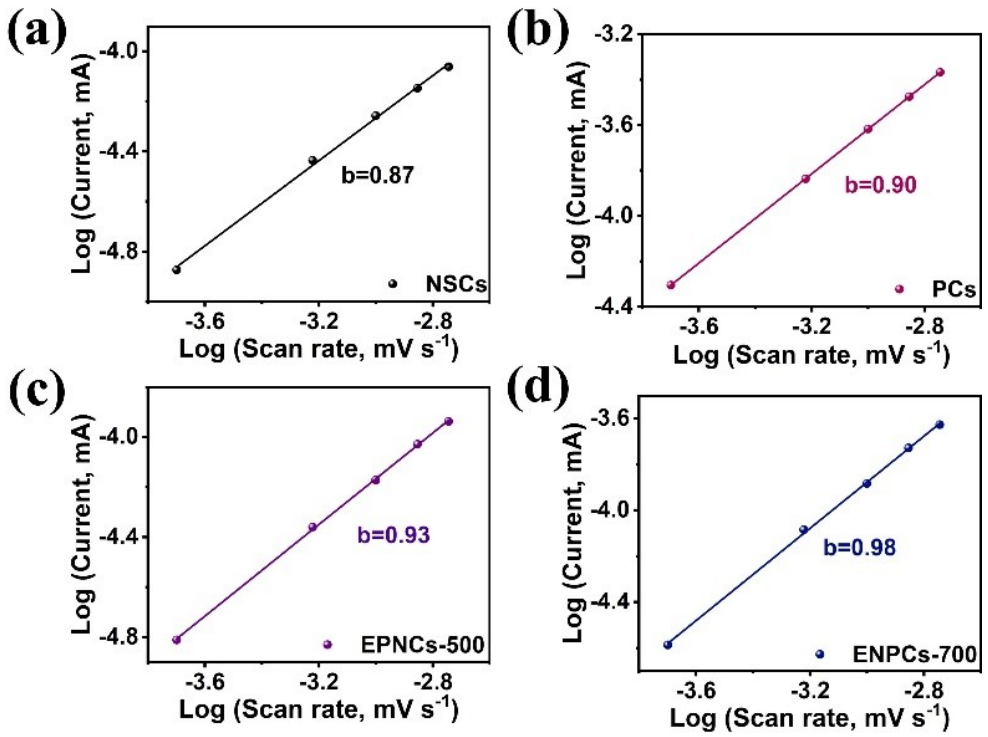

Figure S14. The slope fitting of the b values for (a) PCs, (b) NSCs, (c) ENPCs-500 and (d) ENPCs-700.

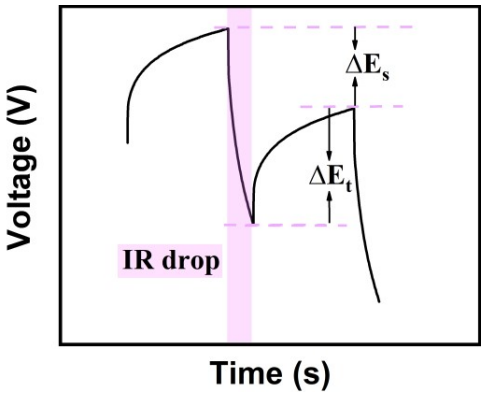

Figure S15. Schematic illustration of the GITT technique.

Galvanostatic intermittent titration technique (GITT) is also employed to study the diffusion coefficients of K-ion in ENPCs-500, ENPCs-600 and ENPCs-700 at 0.1 A g^{-1} for 10 min between rest intervals for 40 min. The diffusion coefficient can be calculated according to Fick's second law as follows[4]:

$$D = \frac{4}{\pi\tau}\left(\frac{m_B V_M}{M_B S}\right)^2\left(\frac{\Delta E_s}{\Delta E_\tau}\right)^2$$

Here, τ is the pulse time, M_B is molar mass of material, m_B and S are the active mass and surface area for the test sample, V_M is the molar volume, ΔE_S and ΔE_τ can be obtained from our test results.

Table S1. the N1s spectra details of ENPCs.

Samples	N content (at%)	N-6 (at%)	N-5 (at%)	N-Q (at%)	O content (at%)	C=O (at%)	C-O (at%)	O=C-OH (at%)
ENPCs-500	2.81	45.4	42.5	12.1	3.83	23.2	38.1	38.7
ENPCs-600	2.57	43.8	38.6	17.6	3.25	27.5	35.9	37.6
ENPCs-700	2.41	42.9	28.7	28.4	2.57	34.6	34.3	31.1

Table S2. Comparison of the potassium storage capacity of ENPCs-600 with previously reported carbon materials.

	Current density ($A\ g^{-1}$)	Cycle number	Specific capacity ($mAh\ g^{-1}$)	References
NPC-600	0.1/1.0	200/3000	219.6/188.7	[5]
NFSC2	0.2/1.0	100/1000	238/186	[6]
FLNG	0.05/0.5	60/500	320/150	[7]
NSO-HCN	0.1/0.5	100/100	209.6/126.4	[8]
NCF700	0.1/1.0	100/300	246.4/104.3	[9]
P-PCNs	0.2/1.0	200/1000	245/184.9	[10]
N-HCNs	0.05/1.0	100/2500	241/154	[11]
ENPCs-600	0.1 5.0	200 5000	381.7 190.1	This work

References

[1] F. C. Zheng, Q. W. Chen, L. Hu, N. Yan and X. K. Kong, *Dalton Trans.,* **2014**, *43*,1220-1227.

[2] G. Kresse and J. Hafner, *Phys Rev B.*, **1993**, *48*, 13115.

[3] J. P. Perdew, K. Burke and M. Ernzerhof, *Phys Rev Lett.*, **1996**, *77*, 3865

[4] X. Wu, Y. L. Chen, Z. Xing, C. W. K. Lam, S. S. Pang, W. Zhang and Z. C. Ju, *Adv. Energy Mater.* **2019**, *9*, 1900343.

[5] J. Li, L. Yu, Y. P. Li, G. R. Wang, L. P. Zhao, B. Peng, S. Y. Zeng, L. Shi and G. Q. Zhang, *Nanoscale* **2021**, 13, 692-699.

[6] Y. L. Zhong, W. X. Dai, D. Liu, W. Wang, L. T. Wang, J. P. Xie, R. Li, Q. L. Yuan, G. Hong, *Small* **2021**, 2101576.

[7] Z. C. Ju, P. Z. Li, G. Y. Ma, Z. Xing, Q. C. Zhuang, Y. T. Qian, *Energy Storage Mater.* **2018**, 11, 38.

[8] M. Chen, Y. P. Cao, C. Ma, H. Yang, *Nano Energy* **2021**, 81, 105640.

[9] L. Li, Y. T. Li, Y. Ye, R. T. Guo, A. N. Wang, G. Q. Zou, H. S. Hou and X. B. Ji, *ACS Nano* **2021**, 15, 6872-6885.

[10] G.B. Zhong, S. Lei, X. Hu, Y. X. Ji, Y. J. Liu, J. Yuan, J. W. Li, H. B. Zhan, and Z. H. Wen, *ACS Appl. Mater. Interfaces* **2021**, 25, 29511-29521.

[11] J. Ruan, X. Wu, Y. Wang, S. Zheng, D. Sun, Y. Song, M. Chen, *J. Mater. Chem. A* **2019**, 7, 19305-19315.